Comparison of raw data based and complex image based sparse SAR imaging methods

Zhilin Xu[123], Bingchen Zhang[12], Hui Bi[4], Chenyang Wu[123], Zhonghao Wei[123], Yirong Wu[1]

1. Institute of Electronics, Chinese Academy of Sciences
2. Key Laboratory of Technology in Geospatial Information Processing and Application System
3. University of Chinese Academy of Sciences, Beijing, 100190, China.
4. Nanyang Technological University, Singapore
Email: bczhang@mail.ie.ac.cn

Abstract—**Sparse signal processing theory has already been introduced to synthetic aperture radar (SAR), which shows potential in improving imaging performance based on raw data or complex image. In this paper, the difference between these two imaging methods is compared and analyzed in detail. It is found that they are equivalent when the raw data is fully sampled. In addition, the performance of the raw data based sparse SAR imaging method is better than the complex image based sparse SAR imaging method when processing in down-sampling data, nonuniform displace phase center sampling, sparse SAR imaging model based azimuth ambiguities suppression.**

Keywords—sparse SAR imaging; lq regularization; azimuth-range decouple; Displaced Phase Center Antenna (DPCA); azimuth ambiguity

I. INTRODUCTION

Synthetic aperture radar (SAR) is an important microwave imaging technology, which has been widely used in agriculture, forestry, oceanic monitoring, topography mapping and military reconnaissance. In recent years, sparse signal processing theory has been introduced to radar imaging, which shows that the sparse observed scene can be reconstructed with less sampled data [1-2]. Compared with matched filtering (MF) based method, sparse signal processing based SAR imaging method can reduce the system complexity and improve the image quality efficiently, such as noise and clutter reduction, sidelobes and azimuth ambiguities suppression [2]. In SAR imaging, Patel *et al*. employed compressive sensing (CS) to recover observed scenes with spotlight SAR data [3]. Cetin *et al*. explored the principle of autofocusing and moving target imaging based on CS [4]. Zhang *et al*. achieved resolution enhancement for inversed synthetic aperture radar (ISAR) imaging via CS [5]. Ender analyzed the reconstruction performance of CS-based wavenumber domain imaging algorithms via the ISAR echo data of satellites [6].

Since the raw data is coupled in azimuth and range directions, the observation matrix based sparse SAR imaging method has huge computational cost, which makes it noneffective in the practical large-scale scene recovery. To solve the problem mentioned above, the azimuth-range decouple based sparse SAR imaging method has proposed in [2] [7], which can reduce the time of imaging efficiently and improve image performance based on the down-sampled raw data for sparse region. The raw data based sparse SAR imaging methods have been widely employed to ScanSAR [8], TOPSAR [9], Sliding Spotlight SAR [10] etc. Quan *et al*. applied sparse signal processing methods to nonuniform displace phase center sampling SAR imaging [11].

Besides, sparse signal processing based imaging method can obtain feature-enhanced radar images [12]. Samadi *et al*. developed an image formation technique that simultaneously enhances multiple types of features [13]. In order to further reduce computational complexity, complex images based sparse SAR imaging method is proposed [14]. The method uses the MF recovered complex image as the input, and then obtain a feature-enhanced SAR image by solving a l_q regularization problem.

In this paper, we discuss the relationship between the raw data based and complex image based sparse SAR imaging methods, and analyze the condition of inequality of those two methods. It shows that they are equivalent when the raw data is fully sampled. In addition, the performance of the raw data based sparse SAR imaging method is better than the complex image based sparse SAR imaging method when processing in down-sampling data, nonuniform displace phase center sampling, sparse SAR imaging model based azimuth ambiguities suppression. Above three cases of SAR data processing can be considered as under-sampling imaging. Furthermore, experiments are carried out in the three under-sampling cases.

The rest of this paper is organized as follows. Section II introduces the raw data based sparse SAR imaging method and the complex image based sparse SAR imaging method. Their relationship is also discussed. Three cases of under-sampling are introduced in Section III. In Section IV, we compared these two sparse SAR imaging methods under three under-sampling cases. Finally, conclusions are drawn in Section V.

II. SPARSE SAR IMAGING MODEL

In this Section, stripmap SAR mode is taken as an example to construct the sparse microwave observation model. Neglecting the displacement in the process of receiving radar signals, the baseband signal echo of all targets in the observed scene can be represented as:

$$y(t,\tau) = \iint\limits_{(p,q)\in C} x(p,q)\omega_a\left(t-\frac{p}{v}\right)\exp\left\{-j4\pi f_c\frac{R(p,q,t)}{c}\right\}$$
$$s\left(\tau-\frac{2R(p,q,t)}{c}\right)dpdq \qquad (1)$$

where t and τ are the indices of azimuth and range time respectively, p and q are the azimuth and range position of the target, $x(\cdot)$ is the backscattered coefficient of the target, $\omega_a(\cdot)$ is the antenna azimuth weighting, and v is the platform speed, c is the speed of light, $s(\cdot)$ is the transmitted signal with carrier frequency f_c, $R(p,q,t)$ is the slant range.

Let $\mathbf{X}$ represents the two-dimensional (2D) matrix whose elements are the backscattering coefficients of the observed scene, $\mathbf{x}=vec(\mathbf{X})$ is the vectorization operation, which means $\mathbf{X}$ will be replaced sequentially by column to a vector. Let $\mathbf{Y}$ represent the 2D echo data, and $\mathbf{y}=vec(\mathbf{Y})$. Considering thermal noise, then the sparse SAR imaging model can be assumed as [2]:

$$\mathbf{y}=\mathbf{\Phi x}+\mathbf{n} \qquad (2)$$

where $\mathbf{\Phi}$ is the observation matrix , which represents the imaging geometry relationship between radar and surveillance region. In the cases of down-sampling, equation (2) can be rewritten as

$$\mathbf{y}=\mathbf{H\Phi x}+\mathbf{n} \qquad (3)$$

where $\mathbf{H}$ is under-sampling matrix. Specifically, in the sparse SAR azimuth ambiguities suppression model, the echo data can be regarded as:

$$\mathbf{y}=\left(\mathbf{\Phi}_{-1},\mathbf{\Phi}_0,\mathbf{\Phi}_{+1}\right)\begin{pmatrix}\mathbf{x}_{-1}\\\mathbf{x}_0\\\mathbf{x}_{+1}\end{pmatrix}+\mathbf{n}=\mathbf{\Phi x}+\mathbf{n} \qquad (4)$$

where $\mathbf{x}_0$ is the unambiguity image of interested area, $\mathbf{x}_{-1}$ and $\mathbf{x}_1$ are the images of ambiguity area, $\mathbf{\Phi}_i(i=-1,0,1)$ are their observation matrixes respectively. When the observation matrix satisfies several conditions, equation (3) can be solved by solving the $l_q(0<q\leq 1)$ regularization problem [15]:

$$\hat{\mathbf{x}}=\min_{\mathbf{x}}\{\|\mathbf{y}-\mathbf{H\Phi x}\|_2^2+\lambda\|\mathbf{x}\|_q^q\} \qquad (5)$$

where λ is the regularization parameter, which is determined by the sparsity of the scene. Equation (5) can be solved by convex optimization algorithms, non-convex optimization algorithms, greedy tracking algorithms and Bayesian reconstruction algorithms, *etc*. After recovery, $\hat{\mathbf{x}}$ should be reshaped into a matrix.

A. Raw Data Based Sparse SAR Imaging

The azimuth-range decouple imaging method is one of raw data based sparse SAR imaging method, which introduces the echo simulation operator $\mathcal{G}(\bullet)$ to replace the observation matrix $\mathbf{\Phi}$, which is the inverse operation of the MF imaging operator $\mathcal{I}(\bullet)$, *i.e.* $\mathcal{G}(\bullet)=\mathcal{I}^{-1}(\bullet)\approx\mathbf{\Phi}$. Then the observation model can be written as [2] [7]:

$$\mathbf{Y}=\mathbf{H}_a\mathcal{G}(\mathbf{X})\mathbf{H}_r+\mathbf{N} \qquad (6)$$

where $\mathbf{Y}$ is raw data, $\mathbf{H}_a$ and $\mathbf{H}_r$ are azimuth and range down-sampling matrix respectively, and $\mathbf{N}$ is noise matrix. The optimization problem (5) can be rewritten as

$$\hat{\mathbf{X}}=\min_{\mathbf{X}}\{\|\mathbf{Y}-\mathbf{H}_a\mathcal{G}(\mathbf{X})\mathbf{H}_r\|_F^2+\lambda\|\mathbf{X}\|_q^q\} \qquad (7)$$

By using the iterative soft thresholding (IST) algorithm, equation (7) can be solved iteratively [16]

$$\mathbf{X}^{(k+1)}=\eta_{\lambda,\mu,q}\left(\mathbf{X}^{(k)}+\mu\mathcal{I}\left(\mathbf{Y}-\mathbf{H}_a\mathcal{G}\left(\mathbf{X}^{(k)}\right)\mathbf{H}_r\right)\right) \qquad (8)$$

where $\eta_{\lambda,\mu,q}(\cdot)$ is the threshold function; μ is the iterative parameter.

B. Complex Image Based Sparse SAR Imaging

Different from raw data based method, the input of this method is MF recovered complex image from fully sampled raw data. Then the feature-enhanced SAR images can be obtained by solving l_q regularization problem. In the following, complex image based sparse SAR imaging method for full- and under-sampled echo data are introduced, respectively [14].

1) Full-sampled data

For the full-sampled data, $\mathbf{H}_a$ and $\mathbf{H}_r$ both are the 1-matrixs. After performing the imaging operator to $\mathcal{I}(\bullet)$ for equation (6), we have

$$\mathcal{I}(\mathbf{Y})=\mathcal{I}(\mathbf{H}_a\mathcal{G}(\mathbf{X})\mathbf{H}_r)+\mathcal{I}(\mathbf{N})$$
$$\Leftrightarrow \mathbf{X}_{MF}=\mathbf{X}+\mathbf{N}' \qquad (9)$$

where $\mathbf{X}_{MF}$ the complex image obtained by MF from raw data, *i.e.* the input of the algorithm, $\mathbf{N}'$ represents the difference between the real scene $\mathbf{X}$ and the complex image, including noise, clutter and sidelobes. Then, according to imaging model shown in (9), we can reconstruct the observation scene by solve the $l_q(0<q\leq 1)$ optimization problem.

$$\hat{\mathbf{X}}=\min_{\mathbf{X}}\{\|\mathbf{X}_{MF}-\mathbf{X}\|_F^2+\lambda\|\mathbf{X}\|_q^q\} \qquad (10)$$

Similarly, using the IST algorithm, the observation scene can be recovered iteratively as [17]:

$$\mathbf{X}^{(k+1)}=\eta_{\lambda,\mu,q}\left(\mathbf{X}^{(k)}+\mu(\mathbf{X}_{MF}-\mathbf{X}^{(k)})\right) \qquad (11)$$

Compared with equation (8), it is found that the sparse SAR imaging method based on the complex image and the sparse SAR imaging method based on the raw data are equivalently when the fully sampled data is available. However, since each step of iteration is based on the image, the imaging and inverse imaging operations in complex image based method can be canceled, hence the computational complexity can be greatly reduced.

2) Under-sampled data

Under-sampling can be defined as the condition that the sampling rate is less than the Nyquist sampling rate. There are several cases of under-sampled in sparse SAR imaging: (1).

down-sampling, (2).nonuniform displace phase center sampling, (3).sparse SAR imaging model based azimuth ambiguities suppression. Similar to above derivation and considering down-sampled data, the imaging model can be expressed as

$$\mathcal{I}(\mathbf{Y}) = \mathcal{I}(\mathbf{H}_a \mathcal{G}(\mathbf{X})\mathbf{H}_r) + \mathcal{I}(\mathbf{N})$$
$$\Rightarrow \mathbf{X}_{MF-De} = \mathcal{I}(\mathbf{H}_a \mathcal{G}(\mathbf{X})\mathbf{H}_r) + \mathbf{N}' \tag{12}$$

where $\mathbf{X}_{MF-De}$ is complex image reconstructed by MF from under-sampled data. In this case,

$$\mathbf{X}_{MF-De} \neq \mathbf{X}_{MF}$$
$$\mathcal{I}\left(\mathbf{H}_a \mathcal{G}\left(\mathbf{X}^{(k)}\right)\mathbf{H}_r\right) \neq \mathbf{X} \tag{13}$$

Due to the under-sampling of raw data, a well-performance image cannot be obtained by the conventional MF algorithm. Besides, performing the under-sampling for the echo simulation operator leads to defocusing when using the imaging operator $\mathcal{I}(\bullet)$. Furthermore, the complex image based sparse SAR imaging method does not equal to the raw data based sparse SAR imaging method.

III. Sparse SAR Imaging With Under-Sampling

A. Down-Sampling

Down-sampling includes uniform down-sampling and random down-sampling in the range and azimuth directions. Uniform down-sampling evenly extracts data in both the range and azimuth directions from raw data. This method could result in degraded imaging performance. The reconstructed image will have ambiguous targets. Random down-sampling randomly extracts data in the range and azimuth directions from raw data. It is a sampling strategy with superior performance in sparse signal processing. When sparse reconstruction is performed, the reconstruction error will distribute in the entire scene like random noise which can be eliminated [18]. The sparse SAR imaging method based on MF recovered complex images from dawn-sampled data cannot obtain well-performance image [14].

B. Nonuniform Displace Phase Center Sampling

The Displaced Phase Center Antenna (DPCA) technology is proposed to achieve high-resolution and wide-swath imaging in single-transmit-multiple-receive multiple channels SAR mode [19]. DPCA radar imaging system allows for an unambiguous recovery of the Doppler spectrum even for a nonuniform sampling of the SAR signal [20]. When the degree of non-uniform sampling is serious, there will still be tiny amounts of azimuth ambiguities in the image after using the matched filter bank to reconstruct the spectrum. If this complex image is used as input, the imaging performance will be affected. Sparse signal processing methods has been applied to nonuniform displace phase center sampling SAR imaging, which is capable of resolving ambiguity and suppressing clutter effectively and is meanwhile insensitive to additive noise [11].

C. Sparse SAR imaging Model based Azimuth Ambiguities Suppression

The spectrum of SAR antenna beam is not banded. Since the spectrum repeats at PRF intervals, the signal components outside this frequency interval fold back into the main part of the spectrum, which will lead to azimuth ambiguities. Azimuth ambiguities are a critical issue in SAR system, especially in spaceborne SAR. Strong ambiguities signals can cause false alarm in the radar image, which affects SAR image interpretation. The ability of azimuth ambiguities suppression is limited via the complex image based sparse SAR imaging. While azimuth ambiguities can be suppressed effectively via the group sparse modeling based approach in which the reflectivity of target is extended as group sparse signal and its components are jointly recovered by l_q regularization method based on raw data [2] [21].

IV. Experiments

To compare imaging performance of the sparse SAR imaging methods based on raw data and complex image, the experiments are carried out under three under-sampling cases respectively. IST algorithm is used for sparse signal reconstruction. The observed scene is sparse in space domain.

A. Down-Sampling

In this part, an English Bay ships region is selected as the scene of interest, and then performs 80% randomly down-sampling for the fully sampled Radarsat-1 echo data, which means that only 80% of the data is available. Fig.1 shows the reconstructed images from down-sampled echo data by MF, the raw data based sparse SAR imaging method, and the complex image based sparse SAR imaging method, respectively. Due to the data down-sampling, it's apparent that MF could not recover the target successfully because of obvious ambiguities and energy dispersion along the azimuth and range direction. Similarly, the complex image based sparse SAR imaging method needs to use MF to recover a complex image, the de-focused MF based image due to down-sampled data further leads to the poor reconstruction performance. However, the raw data based sparse SAR imaging method reconstructs the considered scene successfully, and obtains an image with lower sidelobes and clutter simultaneously. This experiment result shows that the complex image based imaging method does not have the ability of dealing with down-sampled echo data based sparse imaging, compare to the raw data based imaging method.
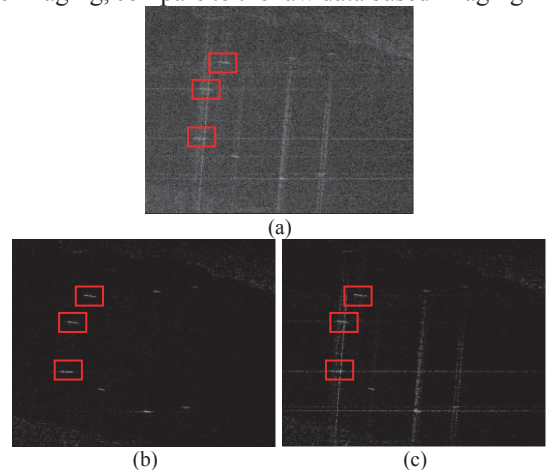
Fig. 1. Images reconstructed from 80% down-sampled echo data by different methods. (a)MF. (b) Raw data based sparse SAR imaging method. (c) Complex image based sparse SAR imaging method

In order to quantitatively evaluate the effects of different algorithms in suppressing image background clutter and noise, target-to-background ratio (TBR) is used as an evaluation index whose definition is shown as

$$TBR(\mathbf{X})=20\log_{10}\left(\frac{\max_{(p,q)\in T}\left|\mathbf{X}_{(p,q)}\right|}{1/N_B\sum_{(p,q)\in B}\left|\mathbf{X}_{(p,q)}\right|}\right) \quad (14)$$

where T is the target area, which is surrounded by the background region B, and N_B is the number of pixels in B. Three ships target in the red frame are selected as the observation area, and its TBR reconstructed by three algorithm are shown in table I

TABLE I   TBR OF TARGET AREA VIA DIFFERENT ALGORITHM WITH DOWNSAMPLED DATA

Imaging algorithm	TBR (dB)		
	Ship1	Ship2	Ship3
MF	30.35	33.44	19.62
Raw data based sparse SAR imaging method	49.14	50.59	43.26
Complex image based sparse SAR imaging method	47.46	46.89	33.39

B. Nonuniform Displace Phase Center Sampling

The echo data used in the experiment are from the single transmit three receive SAR system simulated by the C-band airborne data of the Institute of Electronics of the Chinese Academy of Sciences through re-interpolation. The observed scene was a harbor in Tianjin. Experiments parameters are shown in table II. The imaging results of each algorithm are shown in Fig.2. We can see the performance of different imaging algorithms on noise and clutter reduction, sidelobes and azimuth ambiguities suppression.

TABLE II   EXPERIMENTS PARAMETERS

Parameter	Value
Carrier frequency	5.4GHz
Radar equivalent speed	100m/s
Pulse duration	38 μs
Antenna size	0.9m
Sampling rate in range	750MHz
PRF	768Hz
Number of channels	3

(a)

(b)   (c)
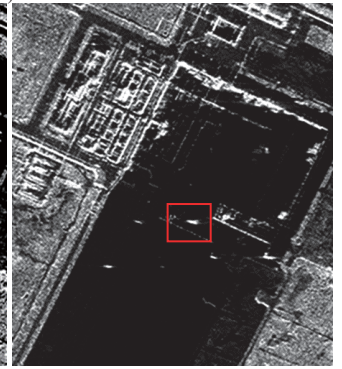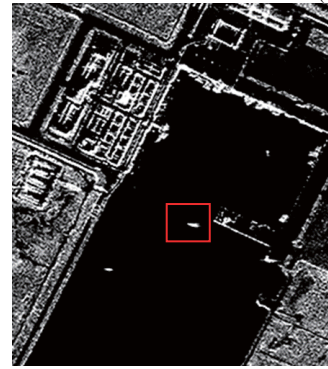
Fig.2 Reconstructed image via different algorithm with single transmit three receive SAR data.(a)MF (b) Raw data based sparse SAR imaging method (c) Complex image based sparse SAR imaging method

The ship target in the red frame of the dock is selected as the observation area, and its TBR reconstructed by three algorithm are shown in table III. It shows that the raw data based sparse SAR imaging method can reduce noise and clutter effectively while the complex image based sparse SAR imaging method cannot achieve the similar performance as the raw data based sparse SAR imaging method.

TABLE III   TBR OF TARGET AREA VIA DIFFERENT ALGORITHM WITH DPCA DATA

Imaging algorithm	TBR (dB)
MF	29.86
Raw data based sparse SAR imaging method	55.37
Complex image based sparse SAR imaging method	36.72

C. Sparse SAR imaging Model based Azimuth Ambiguities Suppression

To compare imaging performance of the imaging methods based on raw data and complex image in azimuth ambiguities suppression, a coastal region is selected as the observed scene from RadarSat-1 data. According to section III, the azimuth spectrum will be aliased in limited PRF conditions due to the azimuth beam pattern. The recovered scenes are shown in Figure 3.

(a)

(b)   (c)
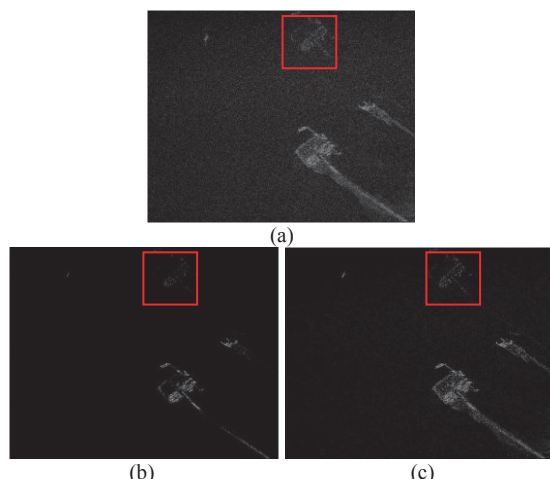
Fig.3 Azimuth ambiguities suppression via different algorithm (a)MF (b) Raw data based sparse SAR imaging method (c) Complex image based sparse SAR imaging method

As in the above two cases, the SAR imaging method based on complex images cannot effectively reconstruct the target. Obvious azimuth ambiguities in the imaging results reconstructed by MF is shown in the red frame of Fig.3 (a), and the average intensity of ghost target is up to -22.86dB. Fig.3 (b) shows that azimuthal ambiguities are effectively suppressed by the raw data based sparse SAR imaging method, and the average intensity of ghost target is down to -34.77dB. The performance of the complex image based sparse SAR imaging method is better than MF but worse than the raw data based sparse SAR imaging method. Ambiguities still exist but the average intensity of ghost target is -28.72dB.

V. CONCLUSION

In this paper, the raw data based sparse SAR imaging method and the complex image based sparse SAR imaging method are compared, and the relationship of two methods are introduced. It shows that two methods are equivalent when the raw data is fully sampled. While, the raw data based sparse SAR imaging method perform better than the complex image based sparse SAR imaging method when processing in down-sampling data, nonuniform displace phase center sampling, sparse SAR imaging model based azimuth ambiguities suppression. The conclusion is well confirmed via experiments under three under-sampling cases.

ACKNOWLEDGMENT

REFERENCES

[1] Potter L C, Ertin E, Parker J T, et al.. Sparsity and compressed sensing in radar imaging[J]. Proceedings of the IEEE, 2010, 98(6): 1006-1020.

[2] Zhang B C, Hong W, Wu Y R. Sparse microwave imaging: Principles and applications[J]. Science China Information Sciences, 2012, 55(8): 1722-1754..

[3] Patel V M, Easley G R, Jr D M H, et al. Compressed Synthetic Aperture Radar[J]. IEEE Journal of Selected Topics in Signal Processing, 2010, 4(2):244-254.

[4] Çetin M, Stojanovic I, Önhon N Ö, et al. . Sparsity-driven synthetic aperture radar imaging: reconstruction, autofocusing, moving targets, and compressed sensing. IEEE Signal Processing Magazine,2014 31(4):27-40.

[5] Zhang L, Xing M, Qiu C W, et al. Resolution Enhancement for Inversed Synthetic Aperture Radar Imaging Under Low SNR via Improved Compressive Sensing[J]. IEEE Transactions on Geoscience & Remote Sensing, 2010, 48(10):3824-3838.

[6] Ender J. . A brief review of compressive sensing applied to radar//2013 14th International Radar Symposium (IRS). Dresden, Germany, 1: 3-16.2013

[7] Fang J, Xu Z, Zhang B, et al. Fast Compressed Sensing SAR Imaging Based on Approximated Observation[J]. IEEE Journal of Selected Topics in Applied Earth Observations & Remote Sensing, 2013, 7(1):352-363.

[8] Bi H, Zhang B, Zhu X X, et al. Azimuth-range decouple-based L 1 regularization method for wide ScanSAR imaging via extended chirp scaling[J]. Journal of Applied Remote Sensing, 2017, 11(1):015007.

[9] Bi H, Zhang B, Zhu X X, et al. Extended Chirp Scaling-Baseband Azimuth Scaling-Based Azimuth–Range Decouple l1 Regularization for TOPS SAR Imaging via CAMP[J]. IEEE Transactions on Geoscience and Remote Sensing, 2017, 55(7): 3748-3763..

[10] Xu Z L, Wei Z H, Zhang B C. 2018. Multichannel sliding spotlight SAR imaging based on sparse signal processing//2018 IEEE International Geoscience and Remote Sensing Symposium (IGARSS).

[11] Quan X, Zhang B, Zhu X X, et al. Unambiguous SAR Imaging for Nonuniform DPC Sampling: lq Regularization Method Using Filter Bank[J]. IEEE Geoscience & Remote Sensing Letters, 2016, 13(11):1596-1600.

[12] Çetin M, Karl W C. Feature-enhanced synthetic aperture radar image formation based on nonquadratic regularization[J]. IEEE Transactions Image Processing, 2001, 10(4):623-631

[13] Samadi S, Çetin M, Masnadi-Shirazi M A. Multiple Feature-Enhanced SAR Imaging Using Sparsity in Combined Dictionaries[J]. IEEE Geoscience & Remote Sensing Letters, 2013, 10(4):821-825.

[14] Bi H, Bi Guoan, Zhang B C, et al. Complex image based sparse SAR imaging and its equivalence. IEEE Transactions on Geoscience and Remote Sensing, 2018. Accepted.

[15] Donoho D L. Compressed Sensing. IEEE Transactions Information Theory, 2006. 52: 1289–1306.

[16] Daubechies I, Defrise M, De Mol C. An iterative thresholding algorithm for linear inverse problems with a sparsity constraint[J]. Communications on pure and applied mathematics, 2004, 57(11): 1413-1457.

[17] Hui Bi, Bingchen Zhang, Zhengdao Wang, and Wen Hong. Lq regularization-based synthetic aperture radar image feature enhancement via iterative thresholding algorithm. Electronics Letters. 2016, 52(15): 1336-1338.

[18] Zhang B C, Zhang Z, Jiang C L, et al. . System design and first airborne experiment of sparse microwave imaging radar: initial results. Science China Information Sciences, 2015.58(6):1-10.

[19] Currie A, Brown M A. 1992. Wide-swath SAR. IEE Proceedings F-Radar and Signal Processing, 139(2):122-135..

[20] Krieger G, Gebert N, Moreira A. Unambiguous SAR signal reconstruction from nonuniform displaced phase center sampling[J]. IEEE Geoscience and Remote Sensing Letters, 2004, 1(4): 260-264.

[21] Zhang B C, Jiang C L, Zhang Z, et al. Azimuth Ambiguity Suppression for SAR Imaging Based on Group Sparse Reconstruction[C]// CoSeRa Bonn. 2013..